Acta Mechanica Solida Sinica, Vol. 27, No. 2, April, 2014 ISSN 0894-9166
Published by AMSS Press, Wuhan, China

HOMOTOPY PERTURBATION SOLUTION AND PERIODICITY ANALYSIS OF NONLINEAR VIBRATION OF THIN RECTANGULAR FUNCTIONALLY GRADED PLATES

A. Allahverdizadeh[1,2⋆] **R. Oftadeh**[2,3] **M. J. Mahjoob**[2] **M. H. Naei**[2]

([1] *School of Engineering - Emerging Technologies, University of Tabriz, Tabriz, Iran*)
([2] *School of Mechanical Engineering, College of Engineering, University of Tehran, Tehran, Iran*)
([3] *Department of Mechanical and Industrial Engineering, Northeastern University, Boston, MA, United States*)

Received 25 April 2012, revision received 22 October 2012

ABSTRACT In this paper nonlinear analysis of a thin rectangular functionally graded plate is formulated in terms of von-Karman's dynamic equations. Functionally Graded Material (FGM) properties vary through the constant thickness of the plate at ambient temperature. By expansion of the solution as a series of mode functions, we reduce the governing equations of motion to a Duffing's equation. The homotopy perturbation solution of generated Duffing's equation is also obtained and compared with numerical solutions. The sufficient conditions for the existence of periodic oscillatory behavior of the plate are established by using Green's function and Schauder's fixed point theorem.

KEY WORDS nonlinear vibration, FGM rectangular plate, Schauder's fixed point theorem, homotopy perturbation method

I. INTRODUCTION

Functionally graded materials (FGMs) are inhomogeneous composite materials and are made from different phases such as ceramic and metal, and also have different applications especially for space vehicles, electronics, and biomedical sectors. FGMs properties vary continuously from one interface to another by gradually varying the volume fraction of constituent materials.

Thin plates are used in many engineering applications, especially in aircraft, space vehicles, automobiles, defense industries, electronics, biomedical engineering, and many engineering structures[1–4]. They are often subjected to severe dynamic loading conditions and can exhibit large amplitude vibrations of the order of the plate thickness. In this case a significant geometrical nonlinearity is induced. Simple models for such oscillations are described with second- and fourth-order partial differential equations. Usually asymptotic methods can be used to construct approximations for solutions of these equations[5].

Many problems in non-linear vibration do not possess exact analytical solutions. One of the most important steps in the theory of non-linear vibration is to establish a sufficient criterion in order to guarantee the existence of periodic solutions. Periodic behavior is the most important regular solution, and has many applications in control of engineering systems. If the system is acted on by a periodic

⋆ Corresponding author. E-mail: allahverdi@ut.ac.ir

force, in the classical theory one expects that the output will also be periodic. Also, the nonlinear resonance theory depends on the assumption that periodic input yields periodic output.

The method of analytic continuation, the process of equating Fourier coefficient, the application of fixed point theorems, and the method of power series are four most frequently used methods of proving the existence of a periodic solution. Here we have used the third method, i.e. Schauder's fixed point theorem, which is of topological character. Schauder generalized the fixed-point theorem of Brouwer for the Banach space. Topological methods often prove applicable in some situations when other methods fail. Although topological methods are not constructive, they guarantee the existence of at least one solution, which is indeed very important[6, 7].

For dynamic behavior of FGMs, Praveen and Reddy[8] conducted the nonlinear transient thermoelastic analysis of functionally graded ceramic–metal plates using FEM. Yang and Shen[1] dealt with the dynamic response of initially stressed FGM rectangular thin plates subjected to impulsive loads. Effects of volume fraction index, foundation stiffness, plate aspect ratio, the shape and duration of impulsive load on the dynamic response of FGM plates have been studied in this work. Gao et al.[9–11] investigated the surface acoustic waves in FGM plates using Homotpy perturbation and layered method. Wang et al.[12] analyzed thickness-shear vibrations in a FGM plate using variation analysis. They showed that in a plate with piecewise constant material properties can support thickness-shear vibration modes and energy trapping is attainable in such a plate. Yang and Shen[13] considered the vibration characteristics and transient response of shear-deformable functionally graded plates made of temperature dependent materials in thermal environments. Differential quadrature technique, Galerkin approach, and the modal superposition method were used to determine the transient response of the plate subjected to lateral dynamic loads. Reddy and Cheng[3] studied the harmonic vibration problem of functionally graded plates by means of a three-dimensional asymptotic theory formulated in terms of transfer matrix. Woo and Meguid[14] investigated the nonlinear analysis of functionally graded plates and shallow shells. An analytical solution has been provided for the coupled large deflection of plates and shallow shells under mechanical load and temperature field. The solution was obtained in terms of Fourier series. Chen[15] analyzed the nonlinear vibration of a shear deformable functionally graded plate by using the equations including the effects of transverse shear deformable and rotary inertia. It was found that the volume fraction of constituents greatly changes the behavior of nonlinear dynamic response. Allahverdizadeh, et al.[16] developed a semi-analytical approach for nonlinear free and forced axisymmetric vibration of a thin circular functionally graded plate. They solved governing equations by using the assumed-time-mode method and Kantorovich time averaging technique.

Many other investigators dealt with various non-linear problems using the fixed-point theorems[17, 18]. Feiz-Dizaji, et al.[19] investigated the flow field of a third-grade non-Newtonian fluid in the annulus of rotating concentric cylinders in the presence of a magnetic field. For this purpose, the constitutive equation of such a fluid flow was simplified, and the existence of the solution to the governing equation was established using Schauder's fixed point theorem. But very little is available on the existence of periodic solution for the response of plates by using the fixed point theorem[20].

In the present paper the Homotopy perturbation solution of generated Duffing's equation is obtained and compared with numerical solutions. Also the determination of the sufficient conditions for the existence of the periodic solution of the initial boundary value problem for simply supported rectangular functionally graded plate via the application of Schauder's fixed point theorem is shown.

II. DERIVATION OF THE GOVERNING EQUATIONS

There are several theories dealing with plates. For thin plates, von-Karman's large deflection theory provides a good approximation and is usually applied[21]. Consider a thin rectangular FGM plate, located in its initially un-deformed configuration by Cartesian coordinates x, y and z. The lengths of the plate, along x and y directions, are a and b, respectively. The z-coordinate is along the uniform thickness h. Figure 1 shows the configuration and coordinate system of this functionally graded rectangular plate. We suppose that the functionally graded plate is made from a mixture of ceramics and metals and the composition varies from the top to the bottom surface, i.e. the top surface ($z = h/2$) of the plate is ceramic-rich whereas the bottom surface ($z = -h/2$) is metal-rich. In such a way, an arbitrary material property P (e.g., Young's modulus E and mass density ρ) can be expressed as

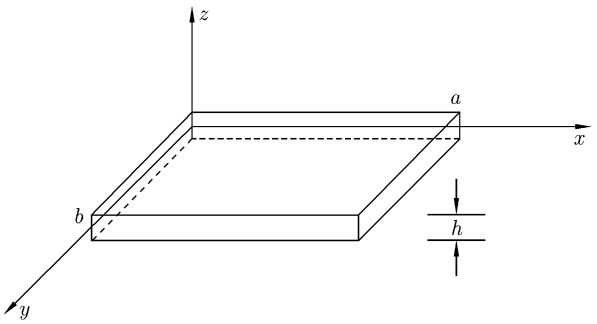

Fig. 1. Configuration and coordinate system of a rectangular plate.

$$P = P_{\mathrm{t}}V_{\mathrm{c}} + P_{\mathrm{b}}V_{\mathrm{m}} \tag{1}$$

where V_{c} and V_{m} are the ceramic and metal volume fractions and are related by

$$V_{\mathrm{c}} + V_{\mathrm{m}} = 1 \tag{2}$$

P_{t} and P_{b} stand for the properties of the top and bottom surfaces of the plate[22]. The volume fraction V_{c} follows a simple power law as

$$V_{\mathrm{c}}(z) = \left(\frac{z}{h} + 0.5\right)^k \tag{3}$$

where the volume fraction index k, dictates the material variation profile across the plate thickness. The Poisson's ratio ν is considered to be 0.3. From Eqs.(1)–(3), one has[23]

$$P(z) = (P_{\mathrm{c}} - P_{\mathrm{m}})\left(\frac{z}{h} + 0.5\right)^k + P_{\mathrm{m}} \tag{4}$$

In what follows, a metal, Stainless Steel ($SUS304$) and ceramics, Silicon Nitride (Si_3N_4) system of FGM is considered, and the mass density and Young's modulus are[24]: $\rho_{\mathrm{c}} = 2370\,\mathrm{kg/m^3}$, $E_{\mathrm{c}} = 322\,\mathrm{GPa}$, $\rho_{\mathrm{m}} = 8166\,\mathrm{kg/m^3}$, $E_{\mathrm{m}} = 207\,\mathrm{GPa}$. The plate is excited in a manner which produces large amplitude vibration with no damping present in the system. By using the Kirchhoff plate theory, the displacements u_x, u_y and u_z are expressed as[25]

$$u_x(x, y, z, t) = u(x, y, t) - zw(x, y, t)_{,x} \tag{5}$$

$$u_y(x, y, z, t) = v(x, y, t) - zw(x, y, t)_{,y} \tag{6}$$

$$u_z(x, y, z, t) = w(x, y, t) \tag{7}$$

where $u(x, y, t)$, $v(x, y, t)$ and $w(x, y, t)$ are the displacements of the point on the middle surface of the plate. The strains at any level z from the neutral plane are obtained by substituting the classical plate deformation kinematics relations in the non-linear strain-displacement relations as

$$\varepsilon_x = u_{,x} + \frac{1}{2}(w_{,x})^2 - zw_{,xx} \tag{8}$$

$$\varepsilon_y = v_{,y} + \frac{1}{2}(w_{,y})^2 - zw_{,yy} \tag{9}$$

$$\gamma_{xy} = v_{,x} + u_{,y} + w_{,x}w_{,y} - 2zw_{,xy} \tag{10}$$

where ε_x and ε_y are the normal strains along the x and y directions, and γ_{xy} is the shear strain. In terms of Hooke's law the stresses are given by

$$\sigma_x = \frac{E(z)}{1 - \nu^2}(\varepsilon_x + \nu\varepsilon_y) \tag{11}$$

$$\sigma_y = \frac{E(z)}{1 - \nu^2}(\varepsilon_y + \nu\varepsilon_x) \tag{12}$$

$$\tau_{xy} = \frac{E(z)}{2(1 + \nu)}\gamma_{xy} \tag{13}$$

where

$$E(z) = E_{\rm cm}\left(\frac{z}{h}+0.5\right)^k + E_{\rm m}, \qquad E_{\rm cm} = E_{\rm c} - E_{\rm m} \tag{14}$$

The in-plane normal forces (N_x, N_y) and in-plane shear force N_{xy} become

$$(N_x, N_y, N_{xy}) = \int_{-h/2}^{h/2} (\sigma_x,\sigma_y,\tau_{xy})\mathrm{d}z \tag{15}$$

In addition, the bending moments (M_x, M_y) and twisting moment M_{xy} become

$$(M_x, M_y, M_{xy}) = \int_{-h/2}^{h/2} (\sigma_x,\sigma_y,\tau_{xy})z\mathrm{d}z \tag{16}$$

These in-plane forces and bending moments are listed in Appendix.

The equation of motion in the z direction can be written as[26]

$$M_{x,xx} + 2M_{xy,xy} + M_{y,yy} = -q - N_x w_{,xx} - 2N_{xy}w_{,xy} - N_y w_{,yy} \tag{17}$$

where q is the transverse load including inertia per unit area of the undeformed mid-plane and can be written as

$$q = f + p - \rho h\ddot{w} - ch\dot{w} \tag{18}$$

where f is the external pressure load, p is the fluid pressure in the case of fluid-structure interaction, $\rho h\ddot{w}$ is the inertia force per unit area and $ch\dot{w}$ is the viscous damping force per unit area.

Now we introduce in-plane stress function F which satisfies the equilibrium equations in x and y directions as

$$N_x = F_{,yy}, \qquad N_y = F_{,xx}, \qquad N_{xy} = -F_{,xy} \tag{19}$$

Substituting Eqs.(52) to (54) into Eq.(18) and doing some manipulations the equation of equilibrium in the z-direction becomes

$$\frac{(AR-B^2)h^3}{A(1-\nu^2)}\nabla^4 w + \left(\rho_{\rm m} + \frac{\rho_{\rm cm}}{k+1}\right)hw_{,tt} = f(x,y,t) + F_{,yy}w_{,xx} - 2F_{,xy}w_{,xy} + F_{,xx}w_{,yy} \tag{20}$$

where coefficients A, B and R are introduced in Appendix.

The compatibility equation is obtained by applying the differential operator $\partial^2/\partial x\partial y$ to Eq.(51):

$$(N_{xy})_{,xy} = \frac{h}{2(1+\nu)}\left[A(u_{,xyy} + v_{,xxy} + w_{,xxy}w_{,y} + w_{,xyy}w_{,x} + w_{,xy}^2 + w_{,xx}w_{,yy}) - 2Bhw_{,xxyy}\right] \tag{21}$$

Using Eqs.(49), (50) and (19), the resulting equation is

$$\nabla^4 F = Ah\left(w_{,xy}^2 - w_{,xx}w_{,yy}\right) \tag{22}$$

Dimensionless variables introduced here are as follows:

$$\begin{aligned} &x^* = \frac{x}{y}, \qquad y^* = \frac{y}{h}, \qquad w^* = \frac{w}{h}, \qquad a^* = \frac{a}{h}, \qquad b^* = \frac{b}{h} \\ &t^* = \frac{\sqrt{E_{\rm m}/\rho_{\rm m}}t}{h}, \qquad f^*(x,y,t) = \frac{f(x,y,t)}{E_{\rm m}}, \qquad F^* = \frac{F}{h^3E_{\rm m}} \end{aligned} \tag{23}$$

and

$$A^* = \frac{A}{E_{\rm m}}, \quad B^* = \frac{B}{E_{\rm m}}, \quad R^* = \frac{R}{E_{\rm m}}, \quad \rho_{\rm cm}^* = \frac{\rho_{\rm cm}}{\rho_{\rm m}}, \quad E_{\rm cm}^* = \frac{E_{\rm cm}}{E_{\rm m}}, \quad \rho_{\rm cm} = \rho_{\rm c} - \rho_{\rm m} \tag{24}$$

Therefore, the governing differential equations for large deflection of rectangular functionally graded plate may be written in non-dimensional form as

$$\frac{AR-B^2}{A(1-\nu^2)}\nabla^4 w + \left(1 + \frac{\rho_{\rm cm}}{K+1}\right)w_{,tt} = f(x,y,t) + F_{,yy}w_{,xx} - 2F_{,xy}w_{,xy} + F_{,xx}w_{,yy} \tag{25}$$

$$\nabla^4 F = A\left(w_{,xy}^2 - w_{,xx}w_{,yy}\right) \tag{26}$$

In these equations, the star symbol has been dropped for convenience. Equations (25) and (26) are dynamic forms of von-Karman's equations, where the longitudinal and rotary inertias are neglected. For homogeneous material, the above relations are identical with Ref.[21]. These governing differential equations are complicated by the obvious nonlinear coupling of membrane and bending theories for thin plates. For simply supported rectangular plate of sides a and b, the boundary conditions on w are

$$\begin{array}{llll} w=0 & \text{and} & \nu w_{,yy}+w_{,xx}=0 & \text{at} \quad x=0,a \\ w=0 & \text{and} & w_{,yy}+\nu\, w_{,xx}=0 & \text{at} \quad y=0,b \end{array} \tag{27}$$

The boundary conditions for in-plane stress function for the case of a plate with stress free edges can be expressed as

$$\begin{array}{llll} F_{,yy}=0 & \text{and} & F_{,xy}=0 & \text{at} \quad x=0,a \\ F_{,xx}=0 & \text{and} & F_{,xy}=0 & \text{at} \quad y=0,b \end{array} \tag{28}$$

And the initial conditions can be written as

$$w(x,y,t)\,|_{t=0}=w_0(x,y), \qquad w(x,y,t)_{,t}\,|_{t=0}=\vartheta_0(x,y) \tag{29}$$

In order to decouple the equations of motion for the dynamics of time dependent amplitudes, an approximate single mode assumption is taken as follows:

$$w(x,y,t)=D(t)\sin\left(\frac{m\pi x}{a}\right)\sin\left(\frac{n\pi y}{b}\right) \tag{30}$$

m and n are integers and $D(t)$ is a dimensionless function of time. The function (30) obviously satisfies the boundary conditions (27). Inserting Eq.(30) in (26) results in

$$\nabla^4 F=\frac{A}{2}\left(\frac{mn\pi^2}{ab}\right)D^2(t)\left[\cos\left(\frac{2m\pi x}{a}\right)+\cos\left(\frac{2n\pi y}{b}\right)\right] \tag{31}$$

Using the Galerkin method, the following solution for the stress function is used to obtain an approximate solution of Eqs.(31) and (25):

$$F=\psi D^2(t)\left[1-\cos\left(\frac{2m\pi x}{a}\right)\right]\left[1-\cos\left(\frac{2n\pi y}{b}\right)\right] \tag{32}$$

The stress free edges boundary conditions (28) are clearly consistent with the assumed solution (33). The expressions for the stress function F and the values for w satisfy the boundary conditions and Eq.(26). However, they do not exactly satisfy Eq.(31). Inserting Eq.(32) into Eq.(31), multiplying the resultant by $[1-\cos(2m\pi x/a)]\,[1-\cos(2n\pi y/b)]$ and integrating over the surface of the plate results in

$$\psi=-\frac{A\left[mn/(ab)\right]^2}{24\left\{\left[(m/a)^2+(n/b)^2\right]^2-4\left[mn/\,(ab)\right]^2/3\right\}^2} \tag{33}$$

Inserting Eqs.(30) and (32) into Eq.(25), multiplying the resulting equation by the corresponding selected mode shape of the lateral displacement, i.e. $\sin(m\pi x/a)\sin(n\pi y/b)$ and integrating over the surface of the plate yields

$$\ddot{D}(t)+PD(t)+QD^3(t)=F(t) \tag{34}$$

in which

$$P=\frac{K}{H}, \qquad Q=\frac{L}{H}, \qquad F(t)=\frac{1}{H}\int_0^b\int_0^a f(x,y,t)\sin\left(\frac{m\pi x}{a}\right)\sin\left(\frac{n\pi y}{b}\right)\mathrm{d}x\mathrm{d}y \tag{35}$$

where

$$\begin{aligned} H&=\frac{a^2b^2}{16\pi^2 mn}\left(1+\frac{\rho_{\mathrm{cm}}}{k+1}\right), \qquad K=\frac{AR-B^2}{A(1-\nu^2)}\frac{a^2b^2\pi^2}{16mn}\left[\left(\frac{m}{a}\right)^2+\left(\frac{n}{b}\right)^2\right]^2 \\ L&=\frac{m^4n^4\pi^4}{24a^3b^3}\frac{A}{\left[(m/a)^2+(n/b)^2\right]^2-4\left[mn/\,(ab)\right]^2/3} \end{aligned} \tag{36}$$

III. HOMOTOPY PERTURBATION SOLUTION

In this section, Eq.(34) will be solved by the Homotopy Perturbation Method[27]. The advantage of this Method compared to other methods such as traditional perturbation method[28] is that this method does not require small parameters in the differential equation. Here, the external force $F(t)$ is taken periodic in the form of $F(t) = \eta\cos(\Omega t + \Phi)$. First, we construct a homotopy as follows[27]:

$$H(v,p) = L(v) - L(u_0) + pL(u_0) + p\left[N(v) - F(t)\right] = 0 \tag{37}$$

where $L(u) = \mathrm{d}^2u/\mathrm{d}t^2 + u$, $N(v)$ constituting the nonlinear term which in this case is $N(v) = Qv^3$, $p \in [0,1]$ is an embedded parameter, and D_0 is an initial approximation of Eq.(34), which satisfies the boundary conditions. The solution of Eq.(34) can be written as a power series in p:

$$v(t) = v_0(t) + pv_1(t) + \cdots \tag{38}$$

Substitution of Eq.(38) into Eq.(37) yields

$$\frac{\mathrm{d}^2v_0}{\mathrm{d}t^2} + Pv_0 - \frac{\mathrm{d}^2D_0}{\mathrm{d}t^2} - PD_0 = 0, \qquad v_0(0) = D_0, \qquad \dot{v}_0(0) = \dot{D}_0 \tag{39a}$$

$$\frac{\mathrm{d}^2v_1}{\mathrm{d}t^2} + Pv_1 + \frac{\mathrm{d}^2D_0}{\mathrm{d}t^2} + PD_0 + Q\,v_0^3 - \eta\cos(\Omega t + \Phi) = 0, \qquad v_1(0) = 0, \qquad \dot{v}_0(0) = 0 \tag{39b}$$

We set $v_0(t)$ as

$$v_0(t) = D_0(t) = D_0\cos(\alpha\,t) + \dot{D}_0\sin(\beta\,t) \tag{40}$$

which is in the form of linear solution of Eq.(34). α and β are unknown constants to be determined later. Substituting $v_0(t)$ and $D_0(t)$ into Eq.(39b), $v_1(t)$ can be readily found as follows:

$$\begin{aligned} v_1(t) = {} & \left(-D_0\alpha^2 + PD_0 + \frac{3QD_0^3}{4} + \frac{3Q\dot{D}_0^2D_0}{2}\right)\frac{\cos(\alpha t)}{\alpha^2 - P} \\ & + \left(-\dot{D}_0\beta^2 + P\dot{D}_0 + \frac{3Q\dot{D}_0^3}{4} + \frac{3QD_0^2\dot{D}_0}{2}\right)\frac{\sin(\beta\,t)}{\beta^2 - P} + \frac{QD_0^3}{4}\frac{\cos(3\alpha t)}{9\alpha^2 - P} \\ & - \frac{Q\dot{D}_0^3}{4}\frac{\sin(3\beta t)}{9\beta^2 - P} + \frac{3QD_0^2\dot{D}_0}{4}\left\{\frac{\sin\left[(2\alpha+\beta)t\right]}{(2\alpha+\beta)^2 - P} - \frac{\sin\left[(2\alpha-\beta)t\right]}{(2\alpha-\beta)^2 - P}\right\} \\ & - \frac{3Q\dot{D}_0^2D_0}{4}\left\{\frac{\cos\left[(2\beta-\alpha)t\right]}{(2\beta-\alpha)^2 - P} - \frac{\cos\left[(2\beta+\alpha)t\right]}{(2\beta+\alpha)^2 - P}\right\} - \frac{\eta\cos(\Omega t + \Phi)}{\Omega^2 - P} \end{aligned} \tag{41}$$

In order to eliminate the secular terms which may occur in the next iteration, we set the coefficients of $\cos(\sqrt{p}t)$ and $\cos(\sqrt{p}t)$ zero which give us two equations. The unknown constants α and β can be found from these equations as follows:

$$\begin{aligned} & \left(-D_0\alpha^2 + PD_0 + \frac{3QD_0^3}{4} + \frac{3Q\dot{D}_0^2D_0}{2}\right)\frac{1}{P - \alpha^2} + \frac{QD_0^3}{4}\frac{1}{P - 9\alpha^2} \\ & \quad - \frac{3Q\dot{D}_0^2D_0}{4}\left[\frac{1}{P - (2\beta - \alpha)^2} - \frac{1}{P - (2\beta + \alpha)^2}\right] - \frac{\eta\cos(\Phi)}{P - \Omega^2} = 0 \end{aligned} \tag{42a}$$

$$\begin{aligned} & \left(-\dot{D}_0\beta^2 + P\dot{D}_0 + \frac{3Q\dot{D}_0^3}{4} + \frac{3QD_0^2\dot{D}_0}{2}\right)\frac{1}{P - \beta^2}\left(\frac{\beta}{\sqrt{P}}\right) - \frac{Q\dot{D}_0^3}{4}\frac{1}{P - 9\beta^2}\left(\frac{3\beta}{\sqrt{P}}\right) \\ & \quad + \frac{3QD_0^2\dot{D}_0}{4}\left[\frac{1}{P - (2\alpha+\beta)^2}\frac{2\alpha+\beta}{\sqrt{P}} - \frac{1}{P - (2\alpha-\beta)^2}\frac{2\alpha-\beta}{\sqrt{P}}\right] - \frac{\eta}{P - \Omega^2}\frac{\Omega}{\sqrt{P}}\sin(\Phi) = 0 \end{aligned} \tag{42b}$$

The explicit solution cannot be found for constants α and β and they should be found numerically for every example. Therefore, the first-order approximation solution can be found by setting $p = 1$ in

Eq.(38) as follows:

$$D(t)=v_0(t)+v_1(t)=\left(\frac{3QD_0^3}{4}+\frac{3Q\dot{D}_0^2D_0}{2}\right)\frac{\cos(\alpha t)}{\alpha^2-P}+\left(\frac{3Q\dot{D}_0^3}{4}+\frac{3QD_0^2\dot{D}_0}{2}\right)\frac{\sin(\beta\,t)}{\beta^2-P}$$
$$+\frac{QD_0^3}{4}\frac{\cos(3\alpha t)}{9\alpha^2-P}-\frac{Q\dot{D}_0^3}{4}\frac{\sin(3\beta t)}{9\beta^2-P}+\frac{3QD_0^2\dot{D}_0}{4}\left\{\frac{\sin\left[(2\alpha+\beta)t\right]}{(2\alpha+\beta)^2-P}-\frac{\sin\left[(2\alpha-\beta)t\right]}{(2\alpha-\beta)^2-P}\right\}$$
$$-\frac{3Q\dot{D}_0^2D_0}{4}\left\{\frac{\cos\left[(2\beta-\alpha)t\right]}{(2\beta-\alpha)^2-P}-\frac{\cos\left[(2\beta+\alpha)t\right]}{(2\beta+\alpha)^2-P}\right\}-\frac{\eta\cos(\Omega t+\Phi)}{\Omega^2-P} \tag{43}$$

For the special case of $\dot{D}(t)=0$, β is equal to zero and the period of solution can be found explicitly as follows:

$$T=\frac{2\pi}{\alpha} \tag{44}$$

where

$$\alpha=\sqrt{\frac{10P+7QD_0^2+\sqrt{64P^2+104PQD_0^2+49Q^2D_0^4}}{18}} \tag{45}$$

The exact period can be obtained as[27]

$$T_{\text{Exact}}=\frac{4}{\sqrt{P+QD_0^2}}\int_0^{\pi/2}\frac{\mathrm{d}\theta}{\sqrt{1-m\sin^2\theta}} \tag{46}$$

To compare the homotopy perturbation solution and exact solution we compare the period when $Q\to\infty$, therefore,

$$\lim_{Q\to\infty}\frac{T_{\text{Exact}}}{T_{\text{HPM}}}=\frac{2\sqrt{7/9}}{\pi}\int_0^{\pi/2}\frac{\mathrm{d}\theta}{\sqrt{1-0.5\sin^2\theta}}=\frac{2\sqrt{7/9}}{\pi}\times 1.8541=1.0414 \tag{47}$$

This result proves that for a finite value of P and any value of Q the maximum relative error constant is less than 4%. for $Q\to\infty$ and $P\to\infty$ we have

$$\lim_{\substack{Q\to\infty\\P\to\infty}}\frac{T_{\text{Exact}}}{T_{\text{HPM}}}=\frac{2}{\pi\sqrt{1+D_0^2}}\sqrt{\frac{10+7D_0^2+\sqrt{64+104D_0^2+49D_0^4}}{18}}\int_0^{\pi/2}\frac{\mathrm{d}\theta}{\sqrt{1-D_0^2\sin^2\theta/[2(1+D_0^2)]}} \tag{48}$$

when P and Q both go to infinity, the ratio depends on D_0. Figure 2 shows the relationship between $T_{\text{Exact}}/T_{\text{HPM}}$ and D_0. As can be seen from this Figure, by increasing the displacement initial value D_0, the maximum relative error constant increases and for $D_0\to\infty$, the ratio converges to 1.0414, which was previously obtained for $Q\to\infty$.

Next, we compare the sample time plot of homotopy perturbation solution and the solution obtained by numerically integrating Eq.(34). The properties of the rectangular plate are set in accordance with the properties in §IV and $D_0=1$. Figure 3 compares the time response of these two solutions. As depicted in this figure, the homotopy perturbation method agrees very well with numerical solution.

IV. PERIODICITY ANALYSIS

Equation (34) belongs to the class of Duffing equations[5]. We assume that $f(x,y,t)$ is odd (even) and periodic in t with period $T=2\pi/\omega$. It is then obvious that $F(t)$ will be periodic with period $T=2\pi/\omega$, and is odd (even). By using Schauder's fixed point theorem, it has been proven that there is an odd (even) periodic solution $D(t)$, such that $D(0)=0$ and $D(-T)=D(T)$ (respectively for even function)[29].

By applying Schauder's fixed point theorem and using the results of Ref.[30] and some manipulations, it is concluded that if $P\geq\omega^2/\pi^2$ or $\omega\leq\pi\sqrt{P}$, no conclusion can be drawn about the existence of periodic solution. If the forcing frequency $\omega>\pi\sqrt{P}$ (where the natural linear resonance frequency is 1) then there is a periodic solution with frequency ω if the amplitude of forcing term $F^*=\max\{|F(t)|:t\in[0,T]\}$ is

$\leq F_0^*$: a limiting value which goes toward 0, as $\omega \to \pi\sqrt{P}$ and goes toward ∞, as $Q \to 0$. By substituting $\omega = 2\pi/T$ in relations, it can be inferred that there is guarantee for the existence of periodic solution when $0 < T^2 P < 4$.

The Fixed Point theorem also guarantees the uniqueness of the solution but it does not mean that under the conditions that the theorem holds the system will not have any bifurcations.

V. PARAMETRIC STUDY

In this section a simply supported rectangular square plate is considered. The plate is 0.2 m in length, 0.2 m in width and 0.005 m in thickness. A parametric study has been carried out with the results given in Figs.4 to 7. The results are obtained for the first mode of vibration (i.e. $m = n = 1$).

First, we study the influence of volume fraction index k and deriving frequency on vibration characteristics of Eq.(34). Figure 4 shows the time response for different k's. The deriving function $F(t)$ of Eq.(34) is taken as $0.01\sin(0.05t)$. As can be seen from this figure, the amplitude and the period of the time response both increase by increasing volume fraction index k. Figure 5 depicts the amplitude of vibration versus k for different driving frequencies. In general, the amplitude increases as the material changes from ceramic to metal (i.e. k increases). In addition, the amplitude decreases by increasing the driving frequency (Ω). Note that all the frequencies used in this figure are greater than $\pi\sqrt{P}$ which guarantees the periodic solution.

Next, the range of the problem parameters for which the existence of periodic solution is guaranteed will be studied. This study is based on the application of the second Shauder's fixed-point theorem and the effects of geometrical (width to thickness ratio) and FGM properties of the plate on the minimum frequency of the distributed load. The results are depicted in Fig.6. The guaranteed domain is the region above all curved lines. It can be inferred from this figure that if the plate is thinner, then the minimum frequency will be smaller and the larger domain will exist.

Figure 7 shows the dependency of the maximum applied vibrating force (F^*) on the distributed load frequency for various volume fraction indices of the FGM plate. It is found that increasing the frequency of the distributed load will increase the domain for applied force in which the periodic response is guaranteed for various volume fraction indicesof the FGM plate. Also it is illustrated that increasing the volume fraction index would result in increasing the maximum allowable vibrating force (F_0^*).

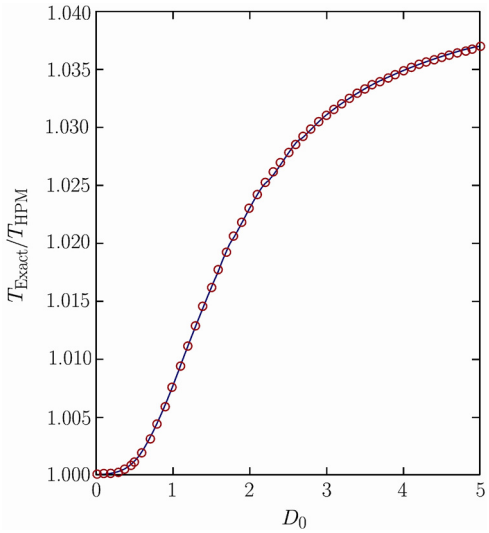

Fig. 2. The relationship between ratio of exact period to homotopy perturbation period ($T_{\text{Exact}}/T_{\text{HPM}}$) and the displacement initial value D_0.

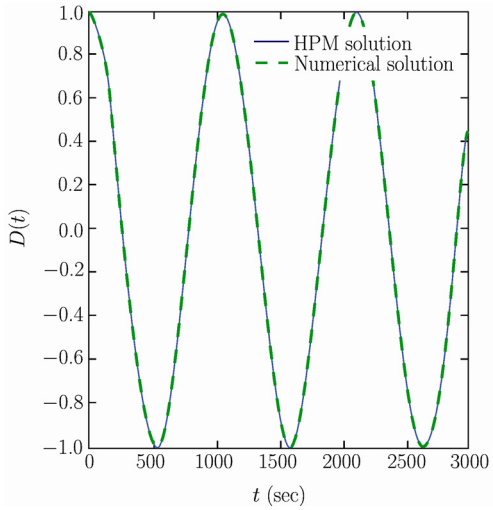

Fig. 3. Comparing time response of homotopy perturbation method and the response obtained by numerically integrating Eq.(34). (free vibration with $D_0 = 1$).

VI. CONCLUSION

For large transverse deflections, a nonlinear analysis of a thin rectangular functionally graded plate has been considered by using the von-Karman's plate theory. In this paper, the periodicity of the nonlinear system is investigated at ambient temperature, and the sufficient conditions for the existence of periodic oscillatory behavior were obtained. It is shown that the governing partial differential equation could be converted into a nonlinear ordinary differential equation. The Homotopy perturbation solution of generated Duffing's equation is also obtained and compared with numerical solutions. The results showed very good agreement with Numerical solution.

Using Green's function and Schauder's fixed point theorem, the conditions for periodic oscillatory behavior of the plate are established and the existence of periodic solution for a Duffing's equation is proved.

The range of the parameters of the problem for the existence of periodic solution is presented and the effects of the FGM properties of the plate as well as the maximum allowable vibrating force to the minimum frequency of distributed load were studied. It is concluded that, the variation of the volume fraction index is influential in FGM properties and the guaranteed domain.

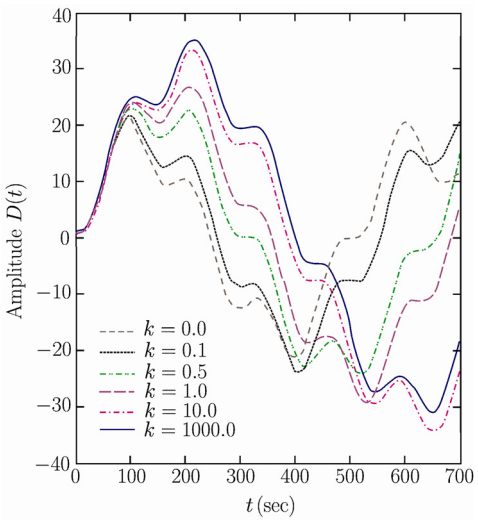

Fig. 4. The influence of volume fraction index k on the time response of Eq.(34) ($F = 0.01\sin(0.05t)$).

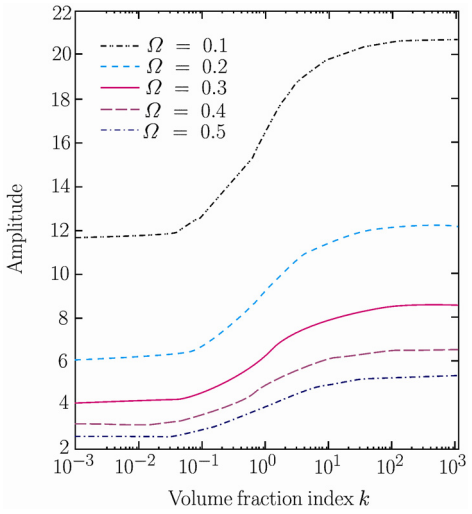

Fig. 5. The influence of volume fraction index k and deriving frequency Ω on the amplitude of vibration ($F = 0.01\sin(\Omega t)$).

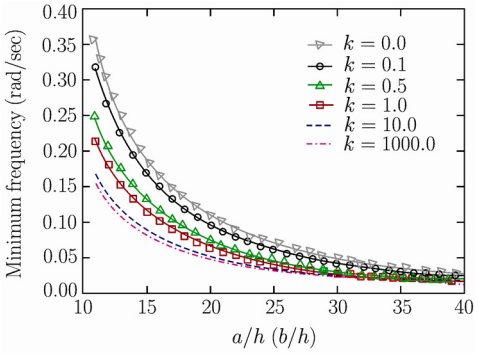

Fig. 6. Minimum frequency of uniform distributed load *vs.* a/h (b/h), in which the existence of periodic solution is guaranteed through this study.

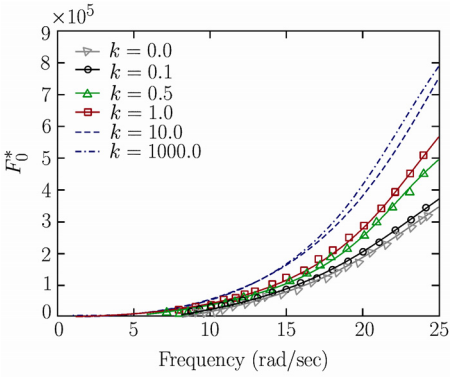

Fig. 7. Dependency of maximum allowable vibrating force on frequency of uniform distributed load and volume fraction index of the FGM plate.

References

[1] Yang,J. and Shen,H.S., Dynamic response of initially stressed functionally graded rectangular thin plates. *Composite Structures*, 2001, 54: 497-508.

[2] Shahrjerdi,A., Mustapha,F., Bayat,M. and Majid,D.L.A., Free vibration analysis of solar functionally graded plates with temperature-dependent material properties using second order shear deformation theory. *Journal of Mechanical Science and Technology*, 2011, 25(9): 2195-2209.

[3] Reddy,J.N. and Cheng,Z.Q., Frequency of functionally graded plates with three-dimensional asymptotic approach. *Journal of Engineering Mechanics*, 2003, 129: 896-900.

[4] Hao,Y.X., Zhang,W., Yang,J. and Li,S.Y., Nonlinear dynamic response of a simply supported rectangular functionally graded material plate under the time-dependent thermal mechanical loads. *Journal of Mechanical Science and Technology*, 2011, 25(7): 1637-1646.

[5] Nayfeh,A.H. and Mook,D.T., Nonlinear Oscillations. New York: Wiley, 1979.

[6] Esmailzadeh,E. and Nakhaie-Jazar,G., Periodic behavior of a cantilever beam with end mass subjected to harmonic base excitation. *International Journal of Non-Linear Mechanics*, 1998, 33: 567-577.

[7] Cronin,J., Fixed Points and Topological Degree in Nonlinear Analysis, Math Survey II. American Mathematical Society, Providence, RI, 1964.

[8] Praveen,G.N. and Reddy,J.N., Nonlinear transient thermoelastic analysis of functionally graded ceramic-metal plates. *International Journal of Solids and Structures*, 1998, 35: 4457-4476.

[9] Gao,L., Wang,J., Zhong,Z. and Du,J., An analysis of surface acoustic wave propagation in functionally graded plates with homotopy analysis method. *Acta Mechanica*, 2009, 208: 249-258.

[10] Gao,L., Wang,J., Zhong,Z. and DU,J., An analysis of surface acoustic wave propagation in a plate of functionally graded materials with a layered model. *Science China Physics, Mechanics and Astronomy*, 2008, 51: 165-175.

[11] Gao,L., Wang,J., Zhong,Z. and DU,J., An exact analysis of surface acoustic waves in a plate of functionally graded materials. *IEEE Transactions on Ultrasonics Ferroelectrics and Frequency Control*, 2009, 56: 2693-2700.

[12] Wang,J., Yang,J. and Li,J., Energy trapping of thickness-shear vibration modes of elastic plates with functionally graded materials. *IEEE Transactions on Ultrasonics Ferroelectrics and Frequency Control*, 2007, 54: 687-690.

[13] Yang,J. and Shen,H.S., Vibration characteristics and transient response of shear-deformable functionally graded plates in thermal environments. *Journal of Sound and Vibration*, 2002, 255: 579-602.

[14] Woo,J. and Meguid,S.A., Nonlinear analysis of functionally graded plates and shallow shells. *International Journal of Solids and Structures*, 2001, 38: 7409-7421.

[15] Chen,C.S., Nonlinear vibration of a shear deformable functionally graded plate. *Composite Structures*, 2005, 68: 295-302.

[16] Allahverdizadeh,A., Naei,M.H. and Nikkhah Bahrami,M., Nonlinear free and forced vibration analysis of thin circular functionally graded plates. *Journal of Sound and Vibration*, 2008, 310: 966-984.

[17] Mehri,B. and Hamedani,G.G., On the existence of periodic solutions of nonlinear second order differential equations. *SIAM Journal on Applied Mathematics*, 1975, 29: 72-76.

[18] Esmailzadeh,E. and Jalili,N., The parametric response of cantilever Timoshenko beams with tip mass under harmonic support motion. *International Journal of Non-Linear Mechanics*, 1998, 33: 765-781.

[19] Feiz-Dizaji,A., Salimpour,M.R. and Jam,F., Flow field of a third-grade non-Newtonian fluid in the annulus of rotating concentric cylinders in the presence of magnetic field. *Journal of Mathematical Analysis and Applications*, 2008, 337: 632-645.

[20] Shadnam,M., Rahimzadeh Rofooei,F., Mofid,M. and Mehri,B., Periodicity in the response of nonlinear plate under moving mass. *Thin-Walled Structures*, 2002, 40: 238-295.

[21] Timoshenko,S. and Woinowsky-Krieger,S., Theory of Plates and Shells, second ed. New York: McGraw-Hill, 1959.

[22] Touloukian,Y.S., Thermo Physical Properties of High Temperature Solid Materials. New York: Macmillan, 1967.

[23] Shafiee,H., Naei,M.H. and Eslami,M.R., In-plane and out-of-plane buckling of arches made of FGM. *International Journal of Mechanical Sciences*, 2006, 48: 907-915.

[24] Reddy,J.N. and Chin,C.D., Thermo-mechanical analysis of functionally graded cylinders and plates. *Journal of Thermal Stresses*, 1998, 21: 593-626.

[25] Brush,D.O. and Almroth,B.O., Buckling of Bars, Plates and Shells. New York: McGraw- Hill, 1975.

[26] Amabili,M., Nonlinear Vibrations and Stability of Shells and Plates. New York: Cambridge University, 2008.

[27] He,J.H., Homotopy perturbation technique. *Computer Methods in Applied Mechanics and Engineering*, 1999, 178: 257-262.

[28] Nayfeh,A.H., Introduction to Perturbation Techniques. New York: Wiley, 1993.
[29] Griffle,D.H., Applied Functional Analysis. New York: Wiley, 1985.
[30] Dizaji,A.F., Sepiani,H.A. and Ebrahimi,F., Allahverdizadeh,A. and Sepiani,H.A., Schauder fixed point theorem based existence of periodic solution for the response of Duffing's oscillator. *Journal of Mechanical Science and Technology*, 2009, 23: 2299-2307.

APPENDIX

These membrane forces and bending moments per unit length for FGM rectangular plate are computed from Eq.(15) and Eq.(16) as follows:

$$N_x = \frac{h}{1-\nu^2}\left\{A\left\{u_{,x}+\frac{1}{2}\left(w_{,x}\right)^2+\nu\left[v_{,y}+\frac{1}{2}\left(w_{,y}\right)^2\right]\right\}-Bh\left(w_{,xx}+\nu w_{,yy}\right)\right\} \tag{49}$$

$$N_y = \frac{h}{1-\nu^2}\left\{A\left\{v_{,y}+\frac{1}{2}\left(w_{,y}\right)^2+\nu\left[u_{,x}+\frac{1}{2}\left(w_{,x}\right)^2\right]\right\}-Bh\left(w_{,yy}+\nu w_{,xx}\right)\right\} \tag{50}$$

$$N_{xy} = \frac{h}{2(1+\nu)}\left[A(u_{,y}+v_{,x}+w_{,x}w_{,y})-2Bh(w_{,xy})\right] \tag{51}$$

$$M_x = \frac{h^3}{1-\nu^2}\left\{-R\left(w_{,xx}+\nu w_{,yy}\right)+\frac{B}{h}\left\{u_{,x}+\frac{1}{2}(w_{,x})^2+\nu\left[v_{,y}+\frac{1}{2}(w_{,y})^2\right]\right\}\right\} \tag{52}$$

$$M_y = \frac{h^3}{1-\nu^2}\left\{-R\left(w_{,yy}+\nu w_{,xx}\right)+\frac{B}{h}\left\{v_{,y}+\frac{1}{2}(w_{,y})^2+\nu\left[u_{,x}+\frac{1}{2}(w_{,x})^2\right]\right\}\right\} \tag{53}$$

$$M_{xy} = \frac{h^3}{2(1+\nu)}\left[-2R\left(w_{,xy}\right)+\frac{B}{h}(u_{,y}+v_{,x}+w_{,x}w_{,y})\right] \tag{54}$$

where

$$A = E_{\mathrm{m}}+\frac{E_{\mathrm{cm}}}{k+1},\qquad B=\frac{kE_{\mathrm{cm}}}{2(k+1)(k+2)},\qquad R=\frac{(k^2+k+2)E_{\mathrm{cm}}}{4(k+1)(k+2)(k+3)}+\frac{E_{\mathrm{m}}}{12} \tag{55}$$